

Dealing with Dead Time Distortion in a Time Digitizer

D. A. Gedcke

Stretching the Dead Time Limits

This study examines the dead time distortions inherent with time digitizers applied to high event rates. It includes a practical scheme for making dead time corrections to the time spectrum after the spectrum has been acquired. The principles are elucidated by the typical application in Time-of-Flight Mass Spectrometry (TOF-MS).

The TOF-MS Example

In Time-of-Flight Mass Spectrometry, ionized molecules are introduced into the acceleration region of the spectrometer, as schematically illustrated in Figure 1. During the injection phase, there is no voltage applied to the acceleration plate. Periodically, the voltage is abruptly increased on the acceleration plate by a pulse that may last a few microseconds. This pulse causes the ionized molecules to accelerate and pass through the grounded grid toward the detector at the remote end of the field-free drift tube. Lighter molecules are accelerated to a higher velocity than heavier molecules. Consequently, the lighter molecules reach the detector more quickly than the heavier molecules. In a simple spectrometer, the flight time, t , from the grounded grid to the detector is related to the mass, m , of the ion, the charge, z , on the molecule and the accelerating voltage, V , by equation (1).

$$t^2 = [s^2 / (2 V)] (m/z) \tag{1}$$

where s is the path length from the grounded grid to the detector.

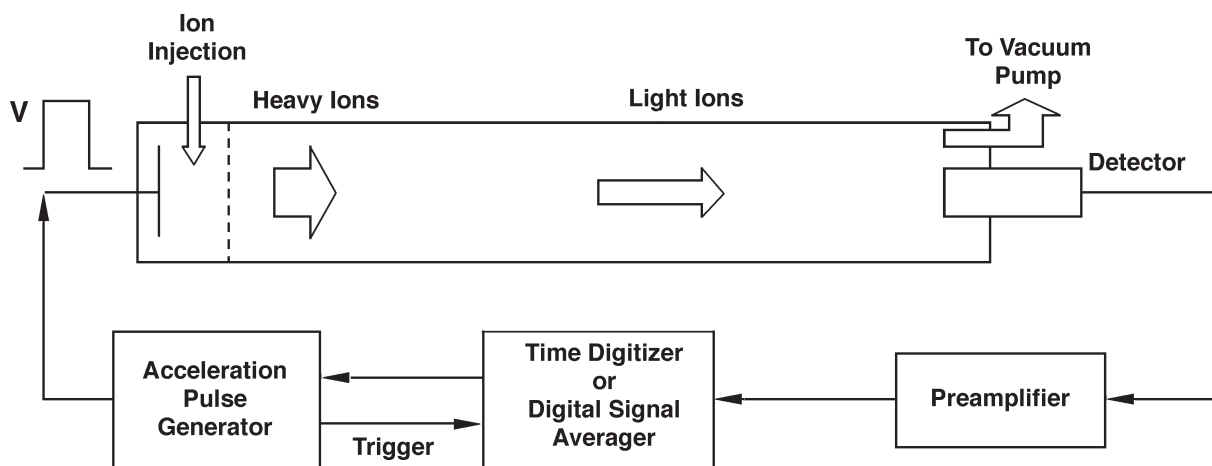


Figure 1. A Simplified Representation of an Electro spray TOF-MS.

When each ion impinges on the detector, it produces a brief pulse at the output of the detector. This pulse is amplified by the preamplifier and presented to the input of the time digitizer. The function of the time digitizer[†] is to measure the arrival time of each ion relative to the time of the most recent acceleration pulse, and to record that value in memory as a digital representation of the flight time of the ion. If the sample being injected into the TOF-MS contains a variety of molecules with different values of m/z , a number of different flight times will be measured following each acceleration pulse, according to the relationship in equation (1). Each acceleration pulse triggers a scan of the time digitizer from zero time to the maximum anticipated flight time. At the end of a scan, the memory contains a record of ion counts versus the time at which each ion was counted. To improve the statistical precision, a large number of scans are implemented in quick succession, and the records from all scans are summed in memory. The result is a spectrum in the form of a histogram. The horizontal axis represents the flight time, and the vertical axis indicates the sum of the ions counted for that specific flight time.

The flight time is recorded as a digital number by capturing the instantaneous value of a digital clock when the pulse arrives at the input to the time digitizer. Typically this clock has a minimum time resolution, e.g., 250 ps per clock tick. Thus, all the events that arrive between clock ticks are assigned the value of the last clock tick. This groups events into bins on the time axis. In the referenced example, the width of the time bin would be 250 ps. This grouping into bins is what causes the spectrum to appear as a histogram.

The Dead Time Handicap

For ions having a specific value of m/z , the arrival times at the detector are statistically distributed. This means there is always some probability that two or more ions will arrive with a spacing that is less than the dead time caused by each ion. Those ions that arrive during the dead time caused by a preceding ion are not counted. This is the source of the dead time losses. As the counting rate increases, close spacing becomes more likely, and the dead time losses increase. Because it is the more closely spaced events that are lost, dead time causes a distortion of the spectrum at high ion arrival rates.

Each ion generates an analog pulse of finite duration at the input to the time digitizer. This is the source of the extending dead time that will be defined shortly. In addition, the digital circuits in the time digitizer cannot respond to pulses that are too closely spaced. This is the origin of the non-extending dead time that is described in more detail below.

One solution to the dead time distortion is to keep the ion rates low enough that the distortion becomes negligible. A second solution is to develop equations that predict the systematic distortion, and to use these equations to correct the distortion after the spectrum has been acquired.

Counting Statistics: The Incentive for Higher Ion Rates

Counting statistics limit the precision in determining peak positions and areas. In turn, this limits the accuracy in determining mass values, isotopic abundance ratios, and concentrations of specific molecules. The random error from counting statistics is also the dominant factor controlling detection limits at low concentrations.

[†]A time digitizer is often referred to as a Time-to-Digital Converter (TDC).

Dealing with Dead Time Distortion in a Time Digitizer

If dead time losses are negligible, the number of ions counted in a peak in the time spectrum is randomly distributed according to the Poisson Distribution^{1, 2}

$$P(N) = \mu^N e^{-\mu}/N! \quad (2)$$

where N is the number of ions counted in a single measurement, $P(N)$ is the probability of observing that specific value of N , and μ is the expected mean value of N that would be obtained by averaging the values of N from an infinite number of repeated measurements. The variance of the Poisson Distribution is

$$\text{Var}(N) = \sigma^2 = \mu \quad (3)$$

The value of N from a single measurement can be used as an adequately accurate estimate of μ . The random error in this estimate will be of the order of σ , where

$$\sigma = \mu^{1/2} \approx N^{1/2} \quad (4)$$

More interestingly, the percent standard deviation in the number of ions in a peak in the time spectrum is given by

$$100\% \times \frac{\sigma}{N} = \frac{100\%}{N^{1/2}} \quad (5)$$

Equation (5) shows that a higher number of ions in the spectrum yields better statistical precision. That fact provides a strong incentive to drive the ion rate as high as possible to minimize the random error.

Consequently, the issue becomes: "How high can the ion rate be pushed before the systematic error caused by dead time losses overwhelms the improvement in the random error in equation (5)?"

The Systematic Error Caused by Dead Time

There are two types of dead time in a time digitizer³:

Extending Dead Time: The arrival of a pulse from an ion causes a dead time interval τ_e . If another pulse arrives during the dead time caused by a preceding pulse, the second pulse is not counted, and the dead time is extended by an additional τ_e from the arrival time of the second pulse. At high counting rates, multiple pulses that are separated by less than τ_e cause considerable extension of the dead time, and a commensurately large dead time loss.

Non-extending Dead Time: The arrival of a pulse causes a dead time interval τ_{ne} . If another pulse arrives during the dead time caused by a preceding pulse, the second pulse is simply not counted. The ignored second pulse has no effect on the dead time.

In both cases, higher counting rates lead to a higher probability of a pulse arriving during the dead time from a previous pulse. Consequently the dead time losses increase with counting rate.

Typically, a time digitizer experiences two dead times in cascade, . . . an extending dead time followed by a non-extending dead time. At the input to the time digitizer, a discriminator threshold is set at a voltage that is large enough to reject noise from the detector and preamplifier, but small enough to accept valid ion pulses. Ion pulses that are large enough to cross this threshold are counted. The width of the analog pulse at the threshold causes an extending dead time. If a second pulse arrives while the first pulse is still above the threshold, the second pulse adds to the first, and extends the dead time by one pulse width from the arrival time of the second pulse. Because the time digitizer counts threshold crossings, it will count only the first pulse. This source of extending dead time is controlled by the pulse shape from the detector, the rise and fall times of the preamplifier, the pulse amplitude, and the discriminator threshold voltage. Typical values of the extending dead time range from 2 ns to 10 ns.

Following recognition of the analog pulse crossing the discriminator threshold, there is typically a non-extending dead time caused by the digital processing circuits in the time digitizer. For the purposes of this study, the start of the non-extending dead time interval is considered to be synchronized with the start of the extending dead time interval. Typical values of the non-extending dead time lie in the range of 0.5 to 50 ns. The throughput equations for the histogram from a time digitizer have been developed previously by Gedcke^{4,5} for the case of an extending dead time followed by a non-extending dead time. The results are summarized in equation (6).

$$\frac{q_i}{n} = \frac{Q_i}{n} \left[\left\{ 1 - U(\tau_{ne} - \tau_e) \sum_{j=i-\tau_{ne}}^{i-\tau_e-1} (q_j/n) \right\} \exp\left(-\sum_{j=i-\tau_e}^{i-1} (Q_j/n)\right) \right] \quad (6)$$

The equation applies to the situation where the counts in the time histogram have been summed for n scans (i.e., n acceleration pulses). The flight time, t , is proportional to the bin number i according to the relation

$$t = i \Delta t \quad (7)$$

where Δt is the width of each time bin, . . . 250 ps in the example previously mentioned. After n scans, bin i contains q_i counts. If there were no dead time losses, bin i should contain Q_i counts. Thus, Q_i/n is the probability of an ion destined for bin i arriving during a single scan, and q_i/n is the probability of observing that ion in a single scan after dead time losses.

To be able to count an ion destined for bin i , there must be no ions arriving in the preceding interval τ_e . The exponential term in equation (6) expresses that probability. This accounts for the losses caused by the extending dead time. The expression in the $\{ \}$ braces is the probability that there are no pulses detected in the preceding time interval τ_{ne} that cause a non-extending dead time. Because the sum in the exponential term has already accounted for zero pulses in the interval $i-1$ to $i-\tau_e$, that interval is excluded from the sum in the non-extending dead time term.* The function

$$\begin{aligned} U(\tau_{ne} - \tau_e) &= 1 \text{ for } \tau_{ne} > \tau_e \\ &= 0 \text{ for } \tau_{ne} \leq \tau_e \end{aligned} \quad (8)$$

ensures that the non-extending dead time will be ignored if it does not extend past the end of the extending dead time interval.

Figure 2 illustrates equation (6) for a specific case of a single peak in the time spectrum with a width of 3 ns at half its height, a 4-ns extending dead time, and a 20-ns non-extending dead time. The bin width is 250 ps. The horizontal axis represents the average number of ions arriving at the detector for that peak during a single scan. In other words, it is the sum of Q_i/n for all bins in the peak. The vertical axis represents the average number of those ions recorded in a single scan by the time digitizer, . . . after dead time losses. The graph indicates that essentially all of the ions are recorded if the average number of ions arriving at the detector for this specific peak in each scan is less than 0.1. As the average number of ions arriving during a single scan increases above 0.1, the curve deviates more and more strongly from a linear relationship. Once the arrival rate reaches 10 ions per scan, increasing the arrival rate no longer increases the recorded number of ions.

* For the purpose of summation in the histogram, τ_e and τ_{ne} are expressed as a number of bins. In other words, the dead time values in nanoseconds are divided by Δt from equation (7) to express the values in number of bins.

Dealing with Dead Time Distortion in a Time Digitizer

A more sensitive picture can be obtained by plotting the difference between the recorded and arriving ions as a percent of the arriving ion rate. This is the percent dead time loss curve shown in Figure 3. If it is not feasible to make dead time corrections to the spectrum, and the goal is to keep dead time losses less than 1%, Figure 3 demonstrates that the average number of arriving ions per scan in the dominant peak must be kept below 0.02.

Not only does the dead time cause a suppression of the area of the peak, but the peak is shifted to lower arrival times as illustrated in Figure 4 for the case where the average arrival rate of ions in the peak is 3. Obviously, the shift in the centroid of the peak will cause an error in the measured value for m/z if left uncorrected. Figure 5 shows the centroid shift as a function of the average ion arrival rate. The shift is expressed as a percent of the full width at half maximum (FWHM) of the peak. From Figure 5, it is obvious that maintaining the average ion arrival rate in the peak less than 0.08 ions per scan will keep the peak shift less than 1% of the FWHM.

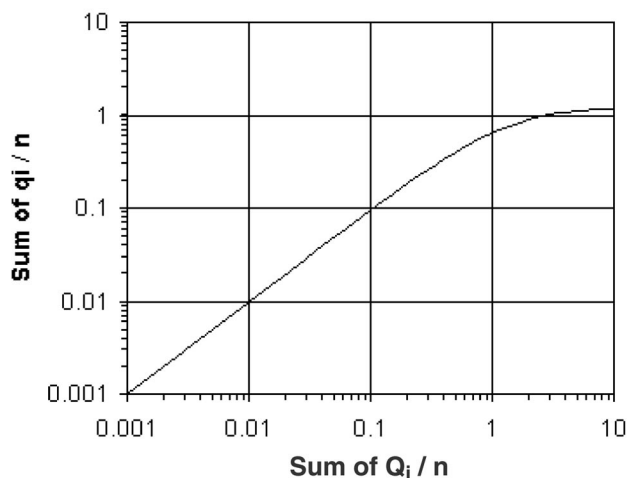


Figure 2. The Throughput Curve from Equation (6) for 4-ns Extending Dead Time Followed by 20-ns Non-Extending Dead Time.

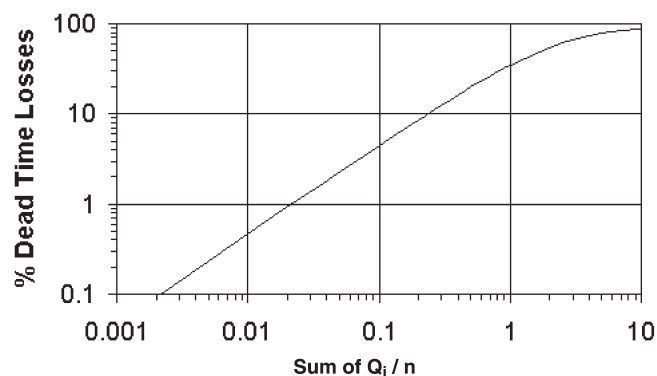


Figure 3. The Percent Dead Time Losses Inherent in Figure 2.

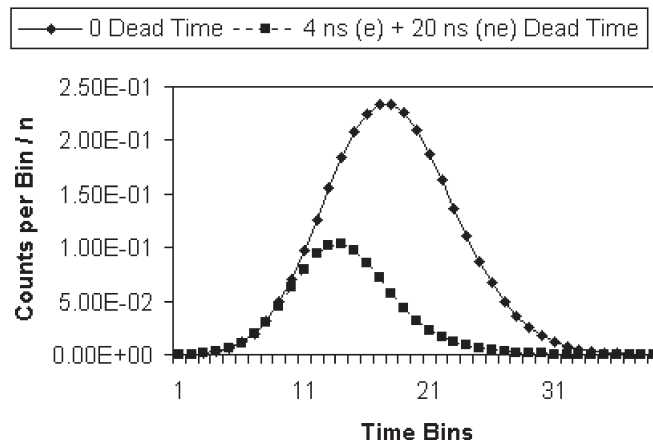


Figure 4. Distortion of the Area and Centroid of the Peak for 66% Dead Time Losses. The horizontal axis is labeled with the bin index i .

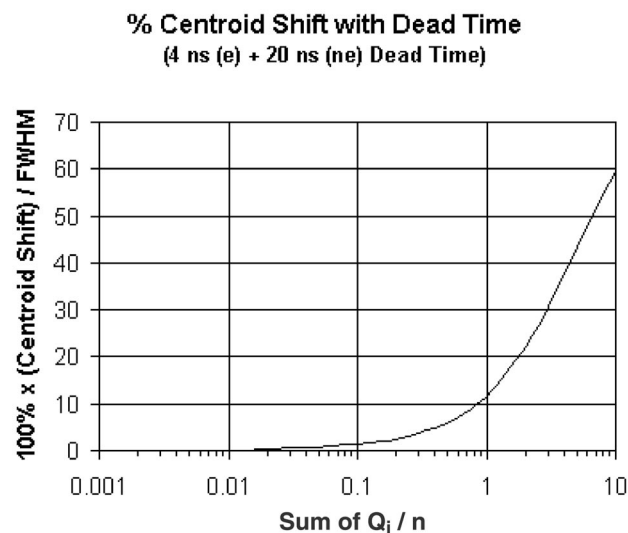


Figure 5. The Centroid Shift of the Peak as a Function of the Average Ion Arrival Rate.

Small Peaks in the Shadows of Large Peaks

Figure 6 shows how the amplitude of a peak can be suppressed if its spacing from a bigger, preceding peak is not larger than the dead time interval. In Figure 6, the area of the smaller, trailing peak is suppressed proportionately more than is experienced by the preceding larger peak. This effect can distort the apparent isotopic abundance ratios. Figure 7 shows how the ratio of the two peak areas varies as the average ion arrival rate per scan in the earlier peak changes. At low rates, where the dead time effects are negligible, the area of the second peak is half the area of the earlier peak. Once the average ion arrival rate in the first peak exceeds 0.1, the ratio begins to deteriorate rapidly with increasing ion rate. When the ion rate surpasses 3, the second peak has essentially disappeared. This effect argues strongly for keeping the average ion arrival rate in the dominant peak less than 0.1 ions per scan. If it is not possible to make dead time corrections, the average ion arrival rate in the dominant peak should be restricted to less than 0.02 ions/scan to keep the distortion of the peak ratios less than 1%.

The Benefits of Reducing the Dead Time

To demonstrate the effects of significantly reducing the dead time, all the computations for Figures 2 through 7 were repeated with the non-extending dead time set to zero, leaving only the 4-ns extending dead time. All other conditions remained the same.

Superficially, the results for a single peak are surprising. The corresponding graphs for Figures 2 through 5 are virtually identical. Because of that lack of distinction, those graphs for 4-ns dead time have been relegated to Appendix A for reference. Upon reflection, it becomes obvious why there is no difference for a single peak between a) 4 ns extending dead time, and b) 4 ns extending dead time and 20 ns non-extending dead time. For each bin in the peak, the preceding 4-ns dead time interval covers most of the significant counts in the peak. Consequently, adding another 16 ns to the tail end of the 4-ns dead time does not significantly increase the counts that are causing dead time.

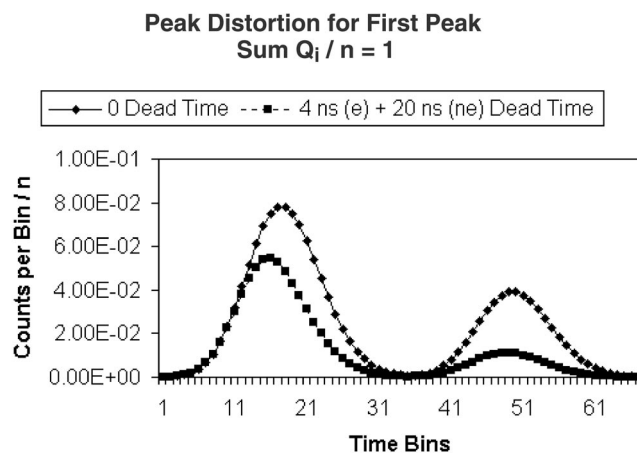


Figure 6. Distortion of a Following Peak by the Dead Time from the Earlier Peak. The horizontal axis is labeled with the bin index i .

Dead Time Effect on Peak Ratios (4 ns Extending + 20 ns Non-extending)

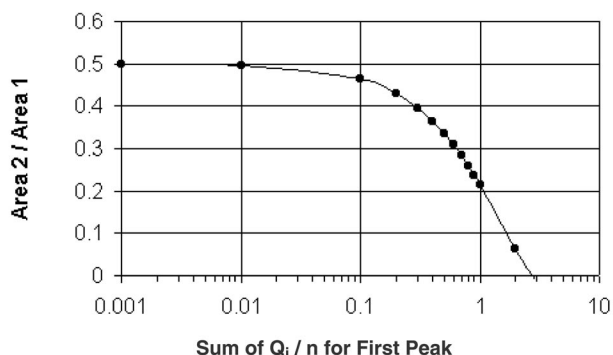


Figure 7. Suppression of the Area of the Second Peak in Figure 6 Relative to the Area of the First Peak as a Result of Dead Time from the First Peak.

However, the case of a small peak closely following a large peak is quite different. Figure 8 illustrates the distortion of the two peaks for an average ion arrival rate of 1 ion/scan in the first peak. With only a 4-ns extending dead time, the area of the first peak is suppressed more than the area of the second peak. This happens because the peak centroids are separated by 8 ns. The peaks are far enough apart, that the dead time caused by the earlier peak does not affect the later peak. But, the ratio of peak areas is still affected by the dead time, . . . just in a different way. Figure 9 shows how the ratio of peak areas is influenced by the average ion arrival rate in the first peak. In the vicinity of 1 ion/scan, the ratio is increasing with ion rate. That happens because the ion rates in the first peak are a factor of 2 larger than in the second peak. Consequently, the percent dead time losses in the first peak are greater than in the second peak.

If it is not possible to make dead time corrections, the average ion arrival rate in the dominant peak should be restricted to less than 0.05 ions/scan to ensure that the error in peak ratios is less than 1%.

Stretching the Limits by Making Dead Time Corrections

If it is not possible to make dead time corrections, the average ion arrival rate per scan in the dominant peak must be limited to <0.08 ions/scan to keep the centroid shift less than 1% of the FWHM of the peak, and <0.02 ions/scan to keep the distortion of peak areas less than 1%. These ceilings on the ion arrival rates can be stretched to much higher limits by making dead time corrections. Here is how the corrections can be accomplished^{4,5,6}.

Equation (6) can be rearranged by multiplying both sides by n and dividing by the term in [] brackets to yield

$$Q_i = q_i \div \left[\left\{ 1 - U(\tau_{ne} - \tau_e) \sum_{j=i-\tau_{ne}}^{i-\tau_e-1} (q_j/n) \right\} \exp\left(-\sum_{j=i-\tau_e}^{i-1} (Q_j/n)\right) \right] \quad (9)$$

After a spectrum has been acquired by summing n scans, the uncorrected values q_i versus the index i reside in the resulting histogram. The corrected histogram (Q_i versus i) is generated by applying equation (9) to the uncorrected histogram, moving from zero time to maximum time, one bin at a time. At each bin, the current value of q_i is combined with the previous values of q_j , the previously calculated values of Q_j , the known value

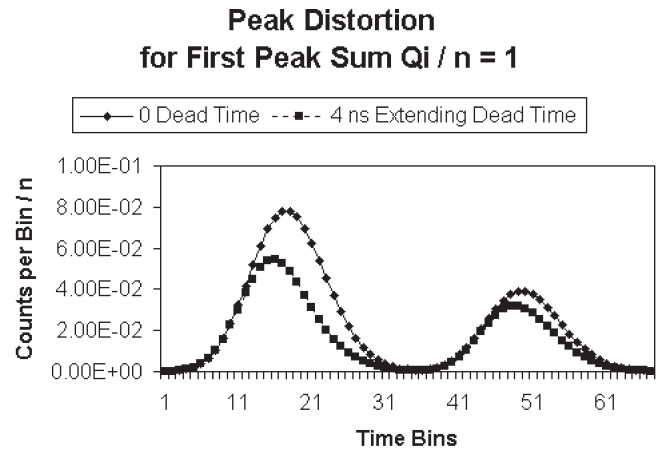


Figure 8. Peak Shape Distortion for Two Closely-Spaced Peaks with a 4-ns Extending Dead Time and an Average Ion Arrival Rate of 1 Ion/Scan in the First Peak. The peak centroids are separated by 8 ns.

Dead Time Effect on Peak Ratios (4 ns Extending Dead Time)

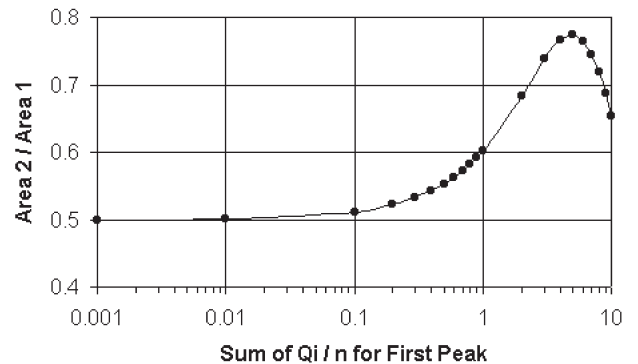


Figure 9. The Ratio of the Second Peak Area to the First Peak Area for Two Closely Spaced Peaks as a Function of the Average Ion Arrival Rate in the First Peak for 4 ns Extending Dead Time.

for n , and the known values of τ_e and τ_{ne} to compute the corrected value Q_i . After passing this algorithm through the histogram from left to right, the spectrum corrected for dead time losses is the array of Q_i values.

At $i = 0$, there is a boundary condition that must be satisfied. Equation (9) requires values of q_j and Q_j for negative values of j . A simple solution is to presume that q_j and Q_j are both zero for negative values of j . If this presumption is not true, Q_i will be underestimated for a few dead time intervals starting from $i = 0$. Beyond that point, the computations for Q_i will have converged to the correct values.

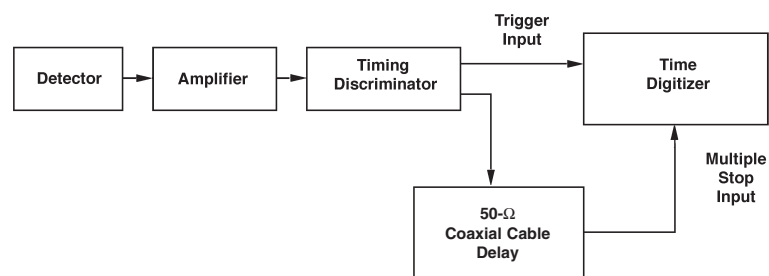
How to Determine τ_e and τ_{ne}

To apply equation (9), reasonably accurate values for τ_e and τ_{ne} must be supplied.

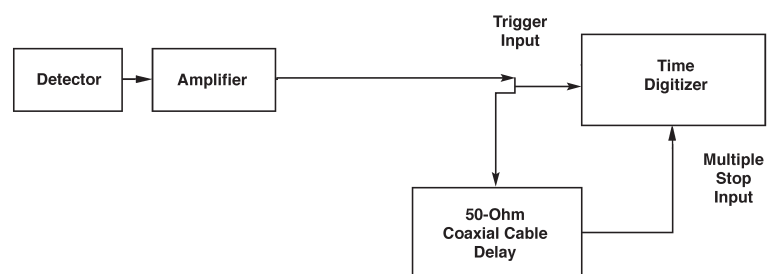
These values can be measured as follows. While the TOF-MS is acquiring spectra, the Trigger Input to the Time Digitizer (see Figure 1) is disconnected, and one of the connections shown in Figure 10 is employed.

Next, the scan length of the Time Digitizer is set at 5 to 10 times the anticipated dead time. Spectra are repeatedly cleared and acquired, while the length of the 50- Ω coaxial cable delay is gradually increased. This adjustment is terminated when the prompt peak shows up at a location that is slightly beyond the dead time caused by the Trigger Input pulse, as illustrated at 4.5 ns in Figure 11. Once the proper delay has been selected, the spectrum is accumulated long enough to yield at least 100 counts per bin in the region that is two dead time intervals to the right of the dominant peak (between 10 and 15 ns in Figure 11). The resulting spectrum represents the probability of observing the time interval t between successive pulses.

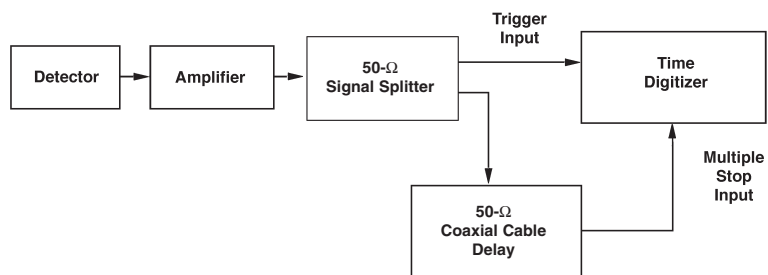
The shape of this time-interval spectrum will depend on the details of the time-of-flight spectrum that is supplying the pulses. (A spectrum with lots of broad, overlapping peaks and a high background is more productive.) Figure 11 depicts the general shape of the result, but does not show the statistical scatter in the counts. Equations (4) and (5) predict that scatter, if the number of counts in a bin is substituted for N .



A. Dual Timing Discriminator Outputs.



B. A Tee at the Time Digitizer High-Impedance Trigger Input.



C. A 50- Ω Signal Splitter.

Figure 10. Three Alternative Configurations for Measuring the Dead Time Interval.

Dealing with Dead Time Distortion in a Time Digitizer

In Figure 11, the large, sharp peak centered at 4.5 ns is caused by the pulse that started the scan at $t = 0$ (via the Trigger Input). Because this triggering pulse is delayed by 4.5 ns and supplied to the Stop Input, it shows up as a Stop pulse at 4.5 ns. The 4.5-ns delay was necessary to get past the shadow caused by the 4-ns dead time that follows the pulse supplied to the Trigger Input.

Once the scan is started by the triggering pulse, additional stop pulses can be recorded, provided that they do not fall in the dead time interval immediately following the triggering pulse. At low counting rates, a Stop pulse arriving at 4.5 ns will be followed by a dead time given by

$$\tau = \tau_e + \tau_{ne} U(\tau_{ne} - \tau_e) . \quad (10)$$

The function $U(\tau_{ne} - \tau_e)$, defined in equation (8), ensures that only the portion of the non-extending dead time that exceeds τ_e will contribute to τ . If the dead time τ is precisely the same for all pulses, the counting rate will be essentially zero during τ , and will jump abruptly to a higher value at the end of τ . The case depicted in Figure 11 is for $\tau_{ne} = 0$ and $\tau_e = 4$ ns. Because the extending dead time varies with the pulse amplitude, there is a range of dead times. That range is exhibited by a gradual increase in the counts from 7 ns to 8 ns in Figure 11. Pragmatically, the dead time τ can be measured from the centroid of the tall peak (at 4.5 ns in Figure 11) to the point at which the counts have recovered to 50% of the final value (at 8.5 ns in Figure 11). This measures the average value of the dead time (4 ns or 16 bins in Figure 11).

If $\tau_e \ll \tau_{ne}$, or $\tau_{ne} \ll \tau_e$, then there is only one type of dead time, and the measurement in Figure 11 completes the task. If neither the extending nor the non-extending component dominates in a system with cascaded dead times, then the portion of τ that is extending must be established. An approximate answer can be gained by recording the analog pulses from the amplifier output with a digital oscilloscope. The oscilloscope must have a bandwidth in excess of 1-GHz to avoid distorting the pulse shapes. Figure 12 illustrates the principle for two different pulse amplitudes. The threshold setting for the discriminator, which sets the lower limit on pulse height for accepted pulses, determines the extending dead time. The width of the analog pulse at this threshold voltage is an estimate of the extending dead time.

It is difficult to obtain an accurate measurement of the extending dead time for several reasons. First of all, the special connections in Figure 10 can perturb the pulse shape, and lead to an inaccurate dead time measurement. Secondly, the dead time depends on the pulse amplitude, as revealed in Figure 12. Even for a specific value of m/z , the microchannel plate detector generates a wide range of pulse heights. The average dead time must be estimated for that range of pulse heights. Furthermore, the average pulse amplitude depends on both m and z . Higher values of m and lower values of z result in lower amplitude pulses from the detector. This can lead to a systematic error in the dead time, and in the dead time correction, as the m/z varies from one end of the time-of-flight spectrum to the other end. One solution to this problem is to insert a non-extending dead time that is large compared to the extending dead time. This makes the dead time virtually independent of pulse amplitude, m and z . The same dead time can be used to accurately correct all parts of the spectrum.

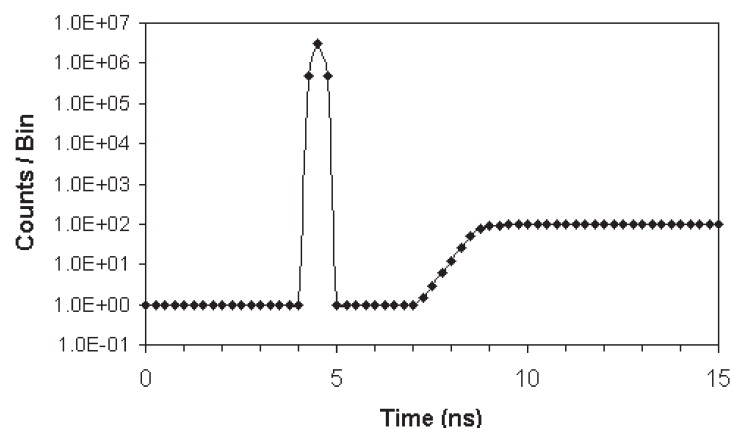


Figure 11. Measuring the Time-Interval Distribution to Determine the Dead Time. The period from 4.5 ns to 8.5 ns is the dead time interval.

Introducing a non-extending dead time

that is large compared to the extending dead time increases the dead time losses. If the dead time losses are restricted to less than 15%, the non-extending dead time can be reduced until it is just slightly longer than the longest extending dead time. This keeps the dead time constant and independent of pulse height, m and z . For dead time losses less than 15% the extending and non-extending dead time equations yield the same result within 1%. Consequently, a pure non-extending dead time can be presumed for the correction, and the measured value of τ from Figure 11 can be inserted for the non-extending dead time.

A brief explanation of the alternatives in Figure 10

is in order. If the Timing Discriminator is a separate module inserted between the Amplifier and Time Digitizer, option A is the much more reliable solution.

Timing Discriminators generally have at least two identical logic pulse outputs. One can be used for the Triggering Input on the Time Digitizer, while the other can be delayed and sent to the Stop Input. Each output can be used without perturbing the other. An ORTEC Model 425A Nanosecond Delay offers a convenient means of adjusting the delay in steps as fine as 1 ns.

Alternative B can be used if the Timing Discriminator is inaccessibly imbedded in the Time Digitizer, provided the Trigger Input has a discriminator that accepts the negative analog inputs, and the input impedance of the Trigger Input is large compared to 50 Ω . The Amplifier output is fed to a BNC Tee on the Trigger Input via a 50- Ω coaxial cable. The other end of the Tee is connected to the delay via another 50- Ω cable. The 50- Ω coaxial impedance must be faithfully preserved from the Amplifier output all the way to the 50- Ω input impedance of the Stop Input. Otherwise, perturbations of the pulse shape will occur.

If the conditions for option B are met, except that the Trigger Input has a 50- Ω input impedance that cannot be changed to a high impedance, then alternative C must be used. In this case, a matched 50- Ω signal splitter is used to preserve a match to the 50- Ω impedance on both Time Digitizer inputs. However, this reduces the analog signal amplitude by a factor of 2. The discriminator thresholds on the Time Digitizer inputs must also be reduced by a factor of 2 to compensate. This will result in some error, because it will be difficult to guarantee an exact match of the factor of 2.

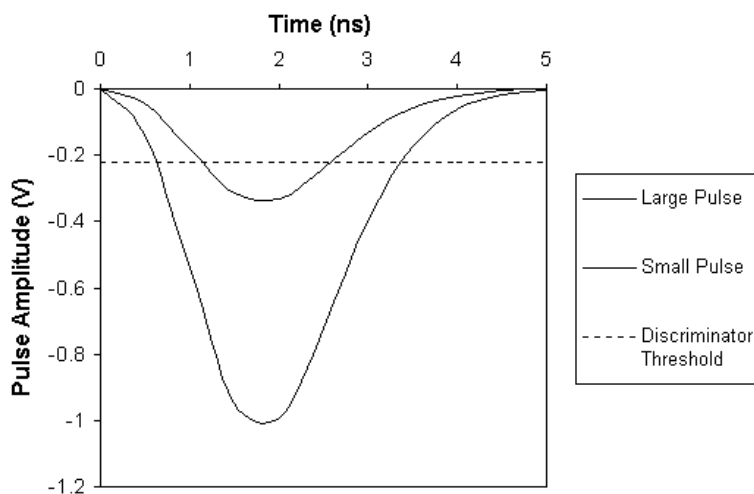


Figure 12. The Extending Dead Time Caused by the Analog Pulse Width at the Discriminator Threshold. Large pulses cause a greater dead time than small pulses.

Sensitivity to Errors in Measuring τ_e and τ_{ne}

In many cases it is difficult to make an accurate measurement of the two components of dead time. Consequently, it is important to assess how sensitive the dead time correction in equation (9) is to an error in the measurement of τ_e and τ_{ne} . Above an average ion arrival rate of 0.1 ions/scan in the dominant peak, it is largely a matter of good or bad luck.

Here is the good-luck case for correcting the area and centroid of a peak for dead time distortion. If the dead time spans most of the peak, and no peak nor significant background precedes the peak within one dead time interval, the dead time correction is virtually impervious to small errors in the specified dead time. For example, the 20-ns non-extending dead time for the case in Figures 2 through 5 was decreased by 10%. This changed the peak area by $<10^{-8}\%$ and the centroid by $<10^{-7}\%$ of the FWHM for ion arrival rates up to 10 ions/scan. Similarly, the 4-ns extending dead time for the case in Figures A-1 through A-4 was increased by 12.5%. This changed the area by $<0.6\%$, and the centroid shifted $<0.6\%$ of the FWHM for ion arrival rates up to 10 ions/scan. The systematic errors in these two cases are negligible, because the dead time spans most of the isolated peak, and there are no significant counts preceding the peak within one dead time interval.

On the other hand, the bad-luck case can be very serious at high ion arrival rates. For the double-peak situation in Figure 8, the extending dead time was reset to 7 ns. This spans the distance from the centroid of the small peak to half-way up the steep slope on the side of the large peak. Next, the dead time was decreased by 12% to 6.25 ns, and the change in area and the shift in the centroid were computed. Figures 13 and 14 show the results. Above an ion arrival rate of 0.1 ions/scan in the dominant peak the error in the area of the smaller peak escalates rapidly, exceeding 10% at 1 ion/scan. Similarly, the centroid shift error grows rapidly above 0.3 ions/scan, reaching 10% of the peak FWHM by 3 ions/scan. Note that this is for a relatively small 12% error in specifying the dead time, and the large peak is only twice the amplitude of the small peak. Larger errors in specifying the dead time and higher peak ratios will magnify the error in the dead time correction.

To avoid errors larger than 1% in the dead time correction, the average ion arrival rate in the dominant peak should be limited to <0.1 ions/scan.

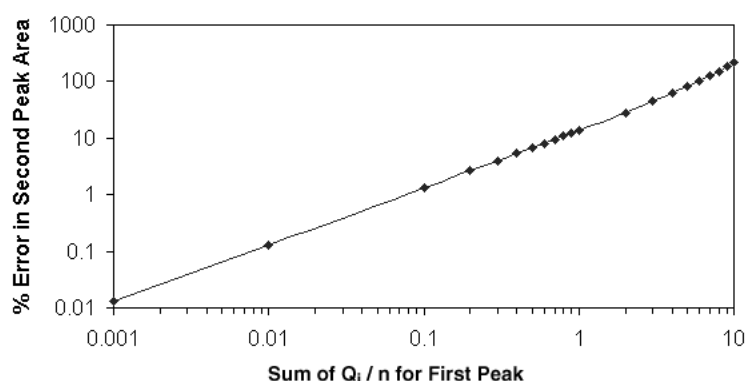


Figure 13. The Sensitivity of the Small Peak Area to a 12% Change in the Extending Dead Time (from 7 ns to 6.25 ns) as a Function of the Average Ion Arrival Rate (Sum of Q_i / n) for the Preceding Large Peak.

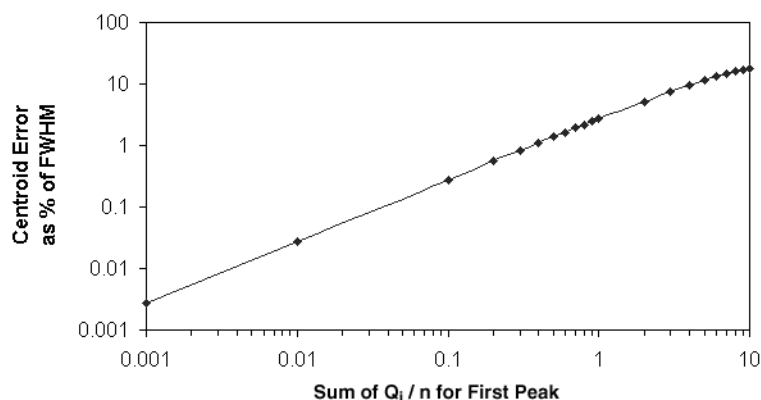


Figure 14. The Same Calculation as in Figure 13, but for the Centroid Shift in the Small Peak as a Percent of the FWHM of the Peak.

The Limit Set by the Random Error

As defined in equations (2) through (5), the number of ions counted in the peak controls the random error in measuring the peak area. Because the random error in each time bin is uncorrelated with the random error in other bins, the random error from Poisson Statistics in each bin also determines the random error in measuring the centroid of the peak. For an isolated peak with a Gaussian shape, the random error in measuring the centroid in the absence of dead time is given by the standard deviation

$$\sigma_c = (\text{FWHM}) / (2.35 N^{1/2}) \quad (11)$$

where FWHM is the Full Width at Half Maximum height of the peak, and N is the number of ions counted in the peak. Clearly, a larger number of ions reduces the random error in measuring the peak position, and this also decreases the random error in measuring the value of m/z for the peak.

Equations (5) and (11) provide a strong incentive for pushing the average ion arrival rate as high as possible to reduce the random errors. However, the dead time effects limit the amount of the improvement. As summarized by Gedcke^{4,5}, Coates⁶ has shown that the variance in the counts in bin i after dead time correction for a non-extending dead time is given by

$$\text{Var}(Q_i) = (\sigma_{Q_i})^2 = k_i Q_i \quad (12)$$

where the magnification factor k_i is given by

$$k_i = R_i + (R_i)^2 (R_i - 1) (q_i/n) \quad (13)$$

and R_i is simply the dead time correction ratio

$$R_i = Q_i/q_i \quad (14)$$

The variance for an extending dead time or cascaded dead times is much more complicated to compute, and closed form equations have not been published to date for these cases.

A more interesting parameter is the percent standard deviation in the corrected counts in bin i as a function of the average ion arrival rate per scan. This is given by

$$\frac{\sigma_{Q_i}}{Q_i} \times 100\% = 100 [(1/q_i) + R_i (R_i - 1) / n]^{1/2} \quad (15)$$

Equation (15) is plotted in Figure 15 for $n = 1,000$ scans, and a 4-ns non-extending dead time. The “Sum of Q_i / n ” is the average ion arrival rate per scan in the peak. As the ion arrival rates are increased on the horizontal axis in Figure 15, the percent standard deviation improves until a minimum is reached in the neighborhood of 1.5 ions/scan. Beyond this point, increasing the ion rate makes the precision worse.

The first term in the [] brackets in equation (15), i.e., $(1/q_i)$, is the contribution from the random error in the number of counts in bin i. The second term, $R_i (R_i - 1) / n$, is the contribution from the random error in the j bins causing the dead time for bin i. As the difference between the dashed and solid lines demonstrates in Figure 15, the second term dominates at high ion rates.

The example computed in Figure 15 is for the bin that contains the highest number of counts at the top of the peak. The shape of the curve in Figure 15 and the position of the minimum will vary with the selected bin and the dead time correction ratio, R_i .

Figure 15 implies that there is little value in increasing the ion rate beyond 1 ion/scan, which corresponds to a dead time correction factor $R_i = 1.6$ in this case.

Guidelines for Managing the Dead Time Effects

Based on the above information, two reasonably safe zones can be defined for managing the dead time effects in a time digitizer according to the following guidelines:

1. In the time spectrum, find the region that contains the largest number of counts, when the width of the region is equal to the dead time. This is the dominant dead time region.
2. If it is not possible to make accurate dead time corrections, maintain the average ion arrival rate in the dominant dead time region <0.02 ions/scan to ensure $<1\%$ distortion of the peak.
3. If reasonably accurate dead time corrections can be made via equation (9), maintain the average ion arrival rate in the dominant dead time region <0.2 ions/scan. This should ensure $<2\%$ distortion in the dead-time corrected peak in most cases.

Generally, guideline 3 corresponds to a dead time correction $<10\%$. With the ORTEC Model 9308, this condition is monitored by the software during the dead time correction process. The software reports the highest correction ratio that was applied, and the bin that experienced that correction ratio. The operator can examine the corrected and uncorrected spectra to see whether the quality of the result is credible.

Completely Eradicating Dead Time Worries

Within the bounds of the above guidelines, equation (9) works quite well for increasing the allowable ion rates by a factor of 10 when the source of ionized molecules has a constant composition and rate during the acquisition of the time-of flight spectrum. But, when the TOF mass spectrometer is fed by the output of a chromatograph, the composition and rate typically change rapidly over the peaks in the chromatograph spectrum. In that case, correction with equation (9) is no longer viable, and the default becomes guideline 2. Unfortunately, the low ion rates in guideline 2, along with the short acquisition times for points on a chromatograph peak ($<<0.5$ seconds), result in a large statistical error and high detection limits.

A much more productive solution is to employ a digital signal averager⁷, such as the ORTEC FASTFLIGHT™. The FASTFLIGHT uses a flash ADC to sample the analog signal from the detector and amplifier. The sample spacing can be as short as 0.5 ns, and this is sufficient to define the shapes of the peaks in the time-of-flight spectrum. Because the detector, amplifier and ADC all respond linearly to the number of ions in a pulse, there is no dead time in recording the ions. Thus, the ion rates can be increased by several orders of magnitude

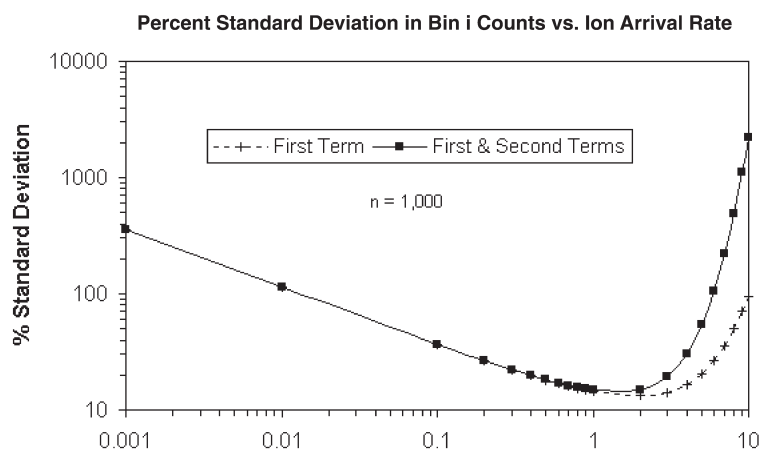


Figure 15. The Graph of Equation 15 Showing a Minimum in the Vicinity of Sum of $Q_i / n = 1.5$

relative to the maximum rates allowed by a time digitizer. With the FASTFLIGHT, the number of ions is limited only by the ion source, the efficiency of the flight path, and the detector response. Consequently, ion detection rates can be improved by a factor ranging from 100 to as much as 5,000. This improves both detection limits and the statistical precision by a factor ranging from 10 to 70. Because there is no dead time, there is no distortion of the isotopic abundance ratios, and no distortions of the m/z values.

For lower ion rates, a time digitizer retains two advantages over the digital signal averager:

- a. If dead times of the order of 50 ns can be tolerated, a time digitizer can deliver exceptional digital time resolution. For example, the ORTEC Model 9308 offers a bin width as fine as 1.2 ps. Current state-of-the-art for digital signal averagers is a 500-ps bin width.
- b. With a time digitizer, the time resolution is not limited by the amplifier pulse width. For a digital signal averager, the typical 1-ns width of the amplifier pulse (FWHM) is convoluted with the 3-ns peak width from the flight path to broaden the peak to 3.16 ns in the recorded spectrum. For most situations in TOF-MS this peak broadening is negligible.

Where dead time losses are a significant problem, a digital signal averager is a superior solution to a time digitizer.

References

1. Ron Jenkins, R. W. Gould, and Dale Gedcke, *Quantitative X-Ray Spectrometry*, Marcel Dekker, New York, First Edition (1981), pp 209 – 229.
2. Phillip R. Bevington, and D. Keith Robinson, *Data Reduction and Error Analysis for the Physical Sciences*, WCB McGraw-Hill, Boston, Second Edition, (1992), pp 23 – 28.
3. Ibid. ref. 1, pp 229 – 244.
4. *1997/1998 EG&G ORTEC Catalog*, pp 2.176 – 2.178
5. *ORTEC Modular Pulse Processing Electronics Catalog (2001)*, PerkinElmer Instruments, Oak Ridge, USA, pp 8.3 – 8.4
6. P. B. Coates, *Rev. Sci. Instrum.* 63 (3), March 1992, p 2084.
7. Ibid. ref. 5, pp 8.41 – 8.49.

Appendix A: Reference Graphs for 4-ns Extending Dead Time

Peak Distortion with 66% Dead Time Losses

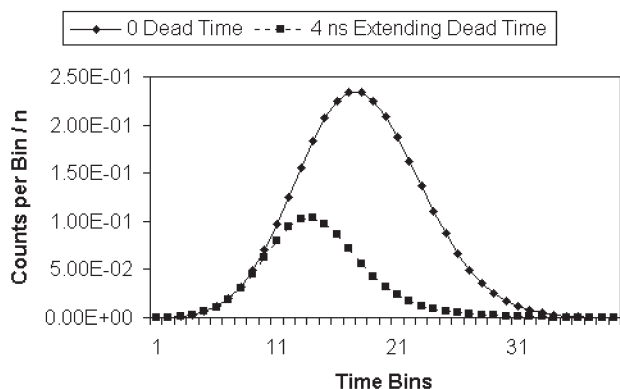


Figure A-1. The Distortion of a Single Peak for an Average Ion Arrival Rate of 3 Ions/Scan and a 4-ns Extending Dead Time. Compare to Figure 4.

Time Digitizer Throughput (4 ns Extending Dead Time)

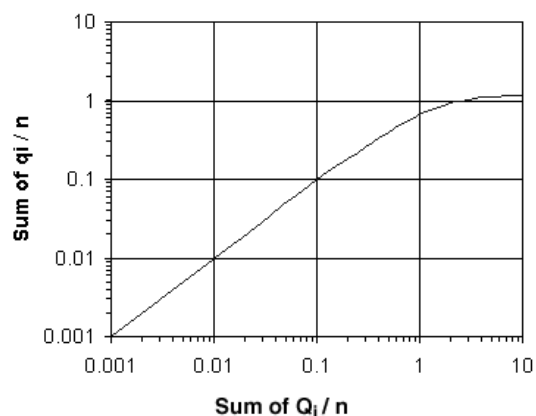


Figure A-2. The Throughput Curve for 4-ns Extending Dead Time. The horizontal axis is the average ion arrival rate in a single scan. The vertical axis is the average number of ions counted per scan after dead time losses. Compare to Figure 2.

Dead Time Losses in a Time Digitizer (4 ns Extending Dead Time)

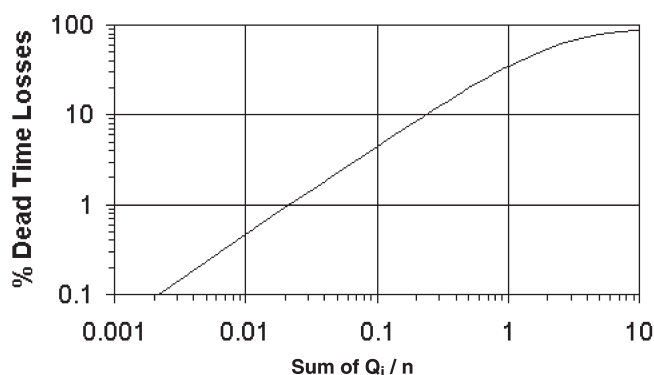


Figure A-3. The Percent Dead Time Losses Corresponding to Figure A-2. Compare to Figure 3.

% Centroid Shift with Dead Time (4 ns Extending Dead Time)

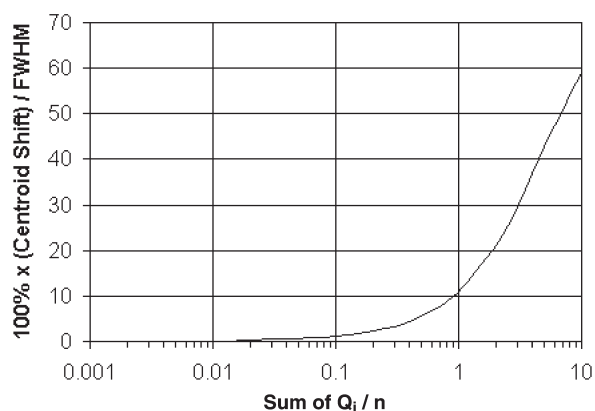


Figure A-4. Centroid Shift as a Percent of the Peak FWHM Versus the Average Ion Arrival Rate and 4-ns Extending Dead Time. Compare to Figure 5.

AN57

Dealing with Dead Time Distortion in a Time Digitizer

Specifications subject to change
062402

ORTEC

800-251-9750 • www.ortec-online.com
info@ortec-online.com • Fax (865) 483-0396
801 South Illinois Ave., Oak Ridge, TN 37831-0895 U.S.A. • (865) 482-4411
For International Office Locations, Visit Our Website

AMETEK
ADVANCED
MEASUREMENT
TECHNOLOGY